JOURNAL OF MATERIALS SCIENCE 27 (1992) 1001–1007

Structural study of semiconducting glassy alloy $As_{0.20}Se_{0.30}Te_{0.50}$

R. A. LIGERO, M. CASAS-RUIZ, J. VÁZQUEZ, P. VILLARES
Facultad de Ciencias, Universidad de Cádiz, Apartamendo 40, Puerto Real, Cádiz, Spain

The radial distribution function (RDF) of the semiconducting glassy alloy $As_{0.20}Se_{0.30}Te_{0.50}$ was obtained by X-ray diffraction. Once the hypotheses on the local order of the alloy had been formulated, the RDF analysis made it possible to evaluate them, referring specifically to the coordination of the As. On this basis, and using the semi-random Metropolis–Monte Carlo method, a structural model was generated whose calculated RDF would agree with the experimental RDF. From this model, structural parameters, such as atomic distances and bond angles between the different possible pairs of atoms in each element, were deduced, and are proposed as a good statistical description of the glass under study.

1. Introduction

Although glass has been known since ancient times, and the Egyptians manufactured glass enamels imitating stones or coating precious metal craft, according to chronicles from 3000 BC, its use has been restricted to passive applications even at the beginning of the twentieth century. Although technology has advanced so spectacularly, it took advantage only of the optical and dielectric properties of glass. Superconductivity and switching phenomena were observed for the first time in the fifties, and began to arouse an enormous interest in scientific circles, for building active elements such as electronic switches, solar cells, memories, chemical catalysts, and special friction-, temperature- and corrosion-resistant materials. This great variety of applications made it necessary to review the concept of glass, its definition and the characteristics that make it different from the rest of solid materials, and the techniques to be used in its manufacture.

Different authors, in recent years, have thus developed definitions which have been rejected by others as not being general enough and sometimes associating the term "glass" with the term "supercooled liquid", excluding materials not obtained by melting, which are increasingly frequent as technology advances (such as electrochemical deposition, vacuum deposition, sputtering, plasma decomposition and ionic implantation). In this sense, the definition given by Britton [1] is especially interesting: "Glass is definable as a material which has the fine structure of a liquid, but the properties of a solid". In any case, the essence of these materials is in their non-periodical structure, in which the atoms can be located in any spatial configuration, being restricted only by the interactions among themselves and by estheric restrictions. That is to say, glass must be considered as the condensed material whose basic characteristic is positional disorder. It is, therefore, a metastable state, although it can maintain its properties for a long time at room temperature.

The atomic structure of these solids is not completely random, as happens with gases, as the cohesion due to their chemical bonds must be present among their atoms [2]. The atoms must be in contact with each other, and there is short-range order. The structural units formed by an atom and its nearest neighbours corresponds, in a way, to the unit cell of a crystal. The atomic distances and bond angles in each of these structural units are not, however, singly determined, but take a certain distribution of values and, unlike in a crystalline network, the repetition of structural units is not periodical, and the orientation and structural characteristics of the clusters is different in each direction. An amorphous solid, therefore, exhibits more variety than a crystal, infinitely increasing the technological possibilities of glasses. The energy of an amorphous material is located in a relative minimum, which is why the obtention processes are based on saving the energetic excess they possess in relation to the same crystalline alloy [3]. Although it was thought that the property of turning into glass was restricted to substances with a very wide band gap, we can now state that this property is common to condensable material in general, if subjected to suitable treatment [4].

The study of glassy material is currently being strongly impulsed by the application of calorimetric techniques; through differential scanning calorimetry (DSC), it is possible to penetrate the glass-forming mechanisms, determining kinetic parameters which describe the phenomena of nucleation and subsequent crystalline growth, from amorphous materials. The knowledge of the factors which influence the glass–crystal reactions leads to a better control of the inverse reactions and, therefore, of the properties and obtention of amorphous materials. An important step will be taken when a definite relationship is found between the structural characteristics and calorimetric magnitudes of glasses; some hypotheses have already been formulated in this sense [5, 6] and verified on

0022–2461

chalcogenide materials. Based on this, and on the fact that the crystallization kinetics of alloy $As_{0.20}Se_{0.30}Te_{0.50}$ have already been studied by ourselves [7], the present work presents a structural analysis of this same alloy.

2. Manufacturing the alloy and preparing the samples for measurement

The alloy to be studied was prepared in bulk, from its highly pure (99.999%) constituent elements, which were mixed homogeneously in adequate proportions, after being pulverized in an agate mortar to grains less than 64 μm in diameter. The powder obtained was introduced into a quartz ampoule, and submitted for two days to an alternating He filling and emptying process, in order to ensure the absence of oxygen inside the ampoule. After the last emptying, in which a value of 10^{-4} Torr was reached, the capsule was sealed with an oxyacetylene burner, and put into a furnace at 650 °C for 24 h, submitted to a longitudinal rotation of 1/3 r.p.m. in order to ensure the homogeneity of the molten material. It was then immersed in a receptacle containing water at 0 °C, in order to solidify the material quickly, avoiding the crystallization of the compound. The ampoule was attacked with hydrofluoridic acid until the quartz walls were weak enough to be broken with a slight pressure without affecting the material inside; a bright grey cylindrical ingot was thus obtained, which presented a large concoid fracture, typical of amorphous materials. The obtained product later proved to be extremely fragile, thus endorsing the method used to extract the sample from the ampoule. If the hammer-and-anvil method, widely used for more resistant alloys, had been used, it would have been impossible to extract the material intact, or even pieces large enough to carry out trustworthy measurements of its density or to make suitable bricks for doing electrical measurements.

A piece of the alloy was cut with a chisel, in order to measure its density using a pycnometric method; a value of $5.3 \pm 0.1\ g\,cm^{-3}$ was obtained, which is slightly under the theoretical value ($5.7\ g\,cm^{-3}$) calculated for the alloy from its composition; this difference is justified by the manufacturing method, which favours the formation of microcavities inside the material.

The rest of the ingot was reduced to powder and sifted to grains under 64 μm in diameter, and a $20 \times 20 \times 1\ mm^3$ brick was made, using a hydraulic press which compressed the material for 10 h, progressively, up to 10000. This brick was submitted to radiation in an automatic Siemens D-500 X-ray diffractometer with a Mo tube, in a scan at a constant angular rate, in order to confirm the amorphous nature of the material.

3. Radial distribution function

Unfortunately, X-ray diffraction techniques do not determine the structure of amorphous solids with the accuracy they do with crystals, and the only thing that can be found by irradiating the samples is the radial distribution function (RDF), which represents the probability of finding two atoms separated by a distance, r [8], and is usually written thus

$$4\pi r^2 \rho(r) \tag{1}$$

where $\rho(r)$ is the average atomic density at a distance r from an arbitrary origin.

When experimental conditions allow us to suppose that the atoms in the sample under consideration have identical probabilities of concentration in space, it is relatively simple to express the RDF in terms of the diffracted intensity, from Debye's diffusion equation [9]

$$I = \sum_i \sum_{j\,(i \neq j)} f_i f_j \frac{\sin sr_{ij}}{sr_{ij}} + N_j \Sigma x_j f_j^2 \tag{2}$$

where I is the intensity, in electronic units, of the radiation diffracted in the direction defined by the scattering vector s, and the summations extend to all the types of atoms in the sample; x_j the atomic fraction of each element in one composition unit, and N the total number of composition units present in the irradiated material; f_j the atomic scattering factor of atom j, and r_{ij} the relative distance between atoms i and j.

Introducing the observable magnitude $i(s)$, called reduced intensity, through

$$i(s) = \frac{I - N\Sigma x_j f_j^2}{\langle f \rangle^2} \tag{3}$$

[10], where $\langle f \rangle = \sum_j f_j x_j$, the interference function $F(s) = s\,i(s)$ is built, such that [9]

$$F(s) = 4\pi \int_0^\infty \Sigma x_j k_j (\rho_j(r) - \rho_0) r \sin sr\, dr \tag{4}$$

where $k_j = f_j / \langle f \rangle$ are the specific scattering factors of each atom, ρ_0 is the average atomic density of the sample and $\rho_j(r)$ is an atomic density function related to atomic type j, defined so that the quantity $\rho_j(r_{ij})\,dV_{ij}$ is the number of atoms in a spherical volume, dV_{ij}, centred on atom i, and whose position in relation to j is r_{ij}.

By calculating the Fourier transformation of this interference function, and bearing in mind that

$$\Sigma x_i k_i = 1 \qquad \Sigma x_i k_i \rho_i(r) = \rho(r) \tag{5}$$

for the radial distribution function

$$4\pi r^2 \rho(r) = 4\pi r^2 \rho_0 + \frac{2r}{\pi} \int_0^\infty s\,i(s) \sin sr\, ds$$

$$= 4\pi r^2 \rho_0 + rG(r) \tag{6}$$

also in terms of the so-called reduced RDF, $rG(r)$.

The diffraction intensities of the alloy in question were measured by four scans in the angular interval from 5° to 110°, time readings being carried out every 0.2° after detecting 4000 impacts on the counter. This procedure makes it possible to work with a constant error, under 1.5%, throughout the scan. In order for the irradiated sample surface to be the same throughout the angular scan, different convergence slits were used in different scan intervals, the measurements

being normalized to a single slit afterwards. The intensities obtained were averaged in the four scans and, by the usual methods [8, 11, 12], corrected of background radiation, polarization and fluorescence effects and multiple scattering.

In order to eliminate the Compton component, which does not supply structural information on the sample, as it does not produce interferences, the values given in the International Tables [13], expressed in electronic units, must be used. The experimental intensities must therefore be normalized to electronic units. The procedure [14] consisted of adjusting the experimental values to the independent radiation calculated for the compound, through two parameters, K_1 and K_2, so that

$$K_1 I_{exp} e^{-K_2 s^2} = \sum x_i f_i^2 + I_{compton} \quad (7)$$

The experimental intensity, normalized to electronic units, is represented in Fig. 1. Once the intensity is obtained in electronic units, it is simple to calculate the reduced intensity, through Equation 3, and the interference function $si(s)$, shown in Fig. 2 for the alloy in question.

Let us observe that the Fourier integral extends throughout the interval [0, ∞] for the scattering vector module; however, we only have experimental data for the angular interval of [5, 110] degrees. The resolution of the integral between the experimental limits leads to a RDF which shows oscillations at its extremes that are not due to structural causes, but to mathematical errors derived from the finite number of terms in the series (series termination error), as may be observed in Fig. 3, which represents the reduced RDF, calculated within the experimental limits. In order to avoid this, a data extension is carried out in the interference function. The literature offers several alternatives for doing this extension; in this case, Shevchick's method was used [15], as it does not cause data alterations in most of the angular interval. Fig. 4 shows the mentioned extension of the interference function, where it is possible to see that the decreasing sinusoidal function derived from the Shevchik method hardly affects the experimental data whose structural information is truly relevant. The Fourier transformation of this $si(s)$ supplies the definite RDF of the compound, shown in Fig. 5.

4. RDF analysis and short-range order

According to the meaning of the RDF, the number of atoms, c, around an arbitrary atom, within the spherical crown of radii a and b, is given by

$$c = \int_a^b 4\pi r^2 \rho(r) dr \quad (8)$$

an expression which is identified with the area under any one of the RDF peaks, if a and b are the limits of the peak.

Considering the first two RDF peaks corresponding to alloy $As_{0.20}Se_{0.30}Te_{0.50}$, the values shown in

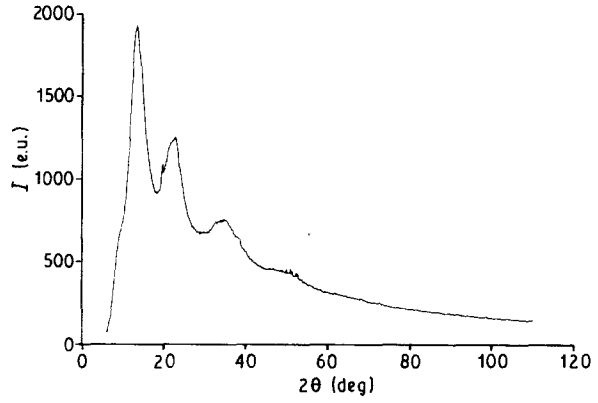

Figure 1 I (e.u.) of the alloy $As_{0.20}Se_{0.30}Te_{0.50}$.

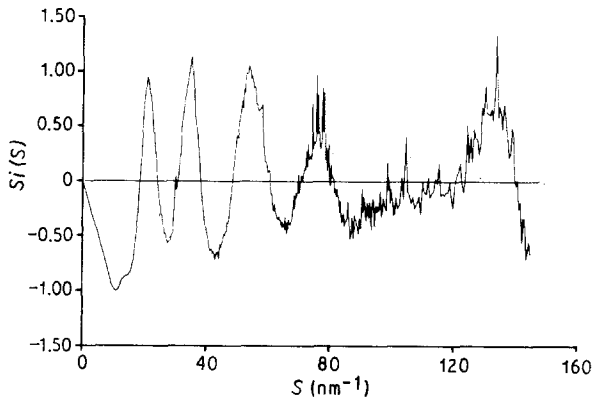

Figure 2 Non-extended $s\,i\,(s)$.

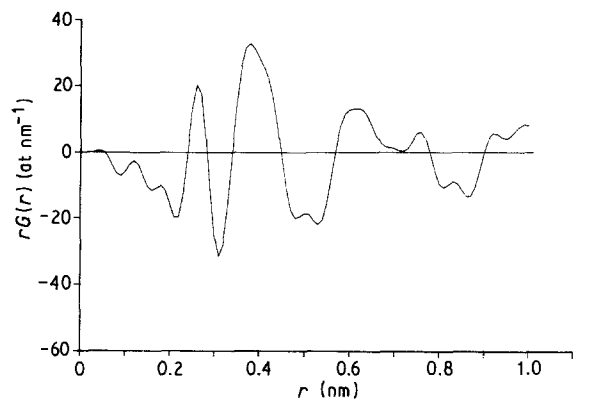

Figure 3 Non-extended $r\,G(r)$.

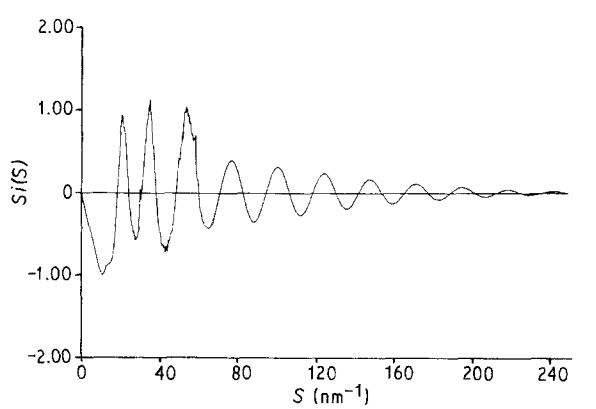

Figure 4 Extended $s\,i(s)$.

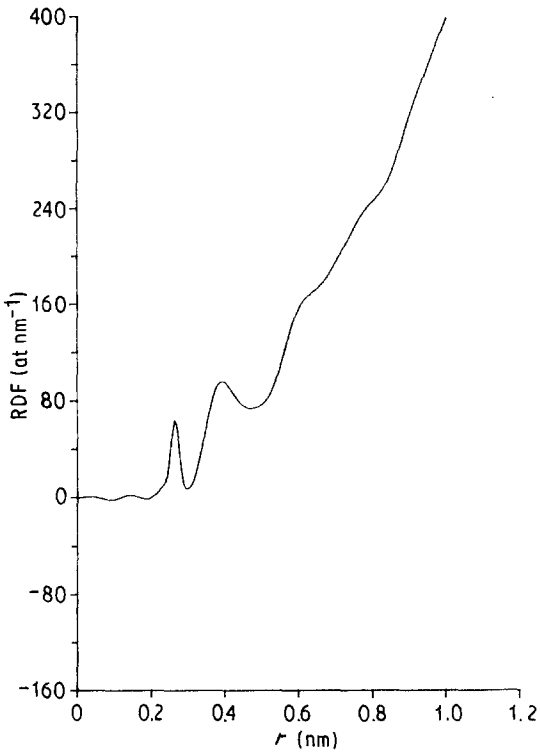

Figure 5 RDF of the model.

TABLE I RDF results

Maximum	1	2
Position (nm)	0.265	0.395
Limits (nm)	0.205–0.290	0.305–0.470
C (at %)	2.1 ± 0.1	—
Average angle (deg)	96.4	—

Table I were found, for the positions and limits of the first and second peak, the average number of atoms in the first coordination sphere of a given atom, c, and the average bond angle, ϕ; the latter was determined from the relationship

$$\phi = 2\sin^{-1}\frac{r_2}{2r_1} \quad (9)$$

The area under the first peak can be expressed in relation to the relative coordinations, n_{ij}, of the different types of atom, n_{ij} being the number of j-type atoms which exist in the first coordination sphere of atom i, as follows [16]:

$$\text{Area} = \frac{2}{\pi}\sum_i\sum_j x_i\frac{n_{ij}}{r_{ij}}\int_a^b rP_{ij}(r)\,dr \quad (10)$$

$P_{ij}(r)$ being a function defined by

$$P_{ij}(r) = \frac{1}{2}\int_0^{s_m}\frac{f_i(s)f_j(s)}{(\Sigma x_i f_i(s))^2}\cos s(r - r_{ij})\,ds \quad (11)$$

Bearing in mind the structural information supplied by the experimental RDF, as well as certain physical–chemical properties of the alloy and their elements, one can postulate on the local order of the glass. These hypotheses, expressed in terms of the relative coordination numbers n_{ij}, and therefore in terms of the number of chemical bonds between the different pairs of atoms in the alloy, a_{ij}, allowed Vázquez *et al.* [17] to find the following relationship:

$$\text{Area} = \frac{1}{50\pi}\left[\left(h + \beta A_{22} - \delta\sum_{i,j\neq 1}A_{ij}\right)N + \alpha A_{22} + \gamma\sum_{i,j\neq 1}A_{ij} + P\left(\sum_{i\neq j\neq 1}A_{ij} - \sum_{\substack{i,j\neq 1\\ i\neq j}}A_{ij}\right)a_{ij}\right]$$

where h, α, β, γ and δ are characteristic parameters of each alloy, N the coordination attributed to a given element of the alloy, π a parameter worth 2 when, in a_{ij}, $i = j$, and -1 when $i \neq j$, and A_{ij} is given by

$$A_{ij} = \frac{1}{r_{ij}}\int_a^b rP_{ij}(r)\,dr \quad (13)$$

In our case, the values of r_{ij} were taken from the literature, according to Table II, and the values of A_{ij}, also shown, were calculated from them.

As, Se and Te are symbolized as elements 1, 2 and 3, respectively and, we chose to single out the element As through N, proposing the following hypotheses. The As may be tri-coordinated or tetra-coordinated in the alloy under study, according to the behaviour proposed for this element in the literature [23–26]. In each case, the relative coordinations of n_{ij} were determined ($i, j \neq 1$) according to the number of Te–Te bonds, a_{33} [18], as well as the characteristic parameters h, α, β, γ and δ, so that it was also possible to calculate the theoretical area under the first RDF peak, A_τ, according to Equation 12. The results are shown in Table III.

TABLE II Bond lengths and A_{ij} parameters

Pair	r_{ij} (nm)	Reference	A_{ij}
As–As	0.249	[19]	0.8284
As–Se	0.238	[20]	0.9135
As–Te	0.262	[21]	1.6232
Se–Se	0.234	[20]	0.9929
Se–Te	0.254	[20]	1.4400
Te–Te	0.271	[22]	2.6731

TABLE III Theoretical results obtained for different coordination hypotheses for the element As

	$N = 3$	$N = 4$
n_{22}	$\frac{-28 + 2a_{33}}{30}$	$\frac{-19 + 2a_{33}}{3}$
n_{23}	$\frac{70 - 2a_{33}}{30}$	$\frac{47.5 - 2a_{33}}{30}$
h	219110	219110
α	−40	−55
β	0	5
γ	100	137.5
δ	0	12.5
A_τ	$1.9991 + 0.01a_{33}$	$1.9140 + 0.01a_{33}$

The theoretically calculated relative coordinations n_{22} and n_{23} must obviously be positive, a fact which restricts the number of Te–Te bonds, a_{33}, present in the alloy, for each of the formulated hypotheses. If the As is tri-coordinated, the interval of values in which a_{33} may oscillate is thus $14 \leqslant a_{33} \leqslant 35$, whereas for tetra-coordinated As, the variation interval for the number of Te–Te bonds is $9.5 \leqslant a_{33} \leqslant 23.75$.

On the other hand, the theoretical areas consequently deduced through each of the formulated hypotheses must be, in all cases, compatible with the experimental value of the first RDF peak, considering the estimated margin of error. This coherence implies a second restriction in the acceptable values of a_{33}. In the present case, as the experimental area was determined as 2.1 ± 0.1 at., the new restrictions are $0.09 \leqslant a_{33} \leqslant 20.9$ and $5.9 \leqslant a_{33} \leqslant 25.9$, for the tri- and tetra-coordinated As hypotheses, respectively.

The superposition of both restrictive conditions for a_{33} finally leads to the conclusion that the variation intervals, for the number of Te–Te bonds, in both coordination hypotheses for the element As, are enclosed by $14 \leqslant a_{33} \leqslant 20.09$ and $9.5 \leqslant a_{33} \leqslant 23.75$. Fig. 6 illustrates this, representing a_{33} in the abscissae, and the band corresponding to the experimental area of the first RDF peak with its margin of error, and the theoretically calculated areas, restricted to the values allowed by the formulated hypotheses, in the ordinates. The degree of overlapping of the latter with the experimental makes it possible to state that both hypotheses are compatible with the experimental measurements, although the tri-coordinated As hypothesis seems less probable, according to the tetra-coordinated As propositions quoted in the literature [23, 24].

These results, derived from the RDF analysis, will strongly condition the structural model proposed forthwith.

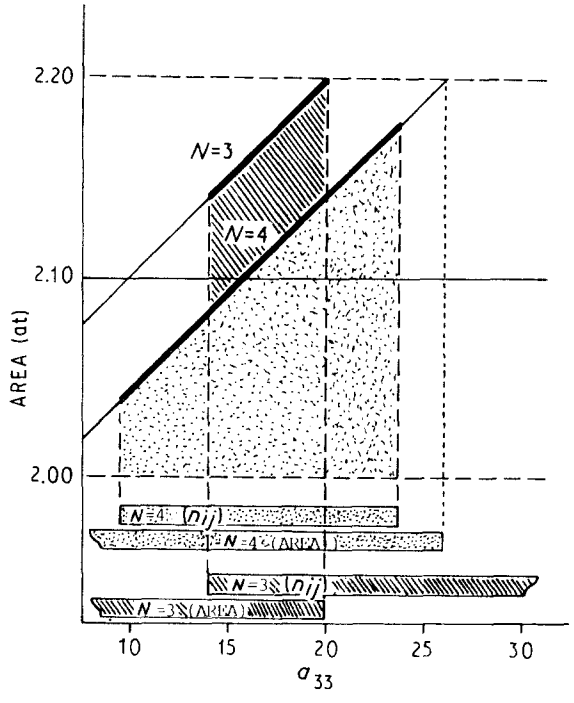

Figure 6 Theoretical area plotted against experimental area.

5. Structural model

There are several random methods for generating structural models of glassy materials [27–30], whose results depend on the manufacturing process used. In this work, the Metropolis–Monte Carlo method [31, 32], based on a random statistical process, was used, as it has proven to be the most suitable for glasses obtained by quenching liquids.

An initial model is taken as a starting point: a spherical volume inside which the corresponding number of atoms, derived from the experimental density measured for the sample, are placed. The positions of these atoms are totally random, save for the restrictions deduced from the experimental RDF analysis, such as the number of atoms in the first coordination sphere, the bond angle between the atoms, or the probability of bonds forming which are compatible with the formulated hypotheses, for the different elements in the alloy. Once the initial configuration is thus obtained, it is possible to calculate its RDF, taking an arbitrary atom as reference, measuring the number of atoms of each kind at predetermined distances from the first, and repeating the process until all the atoms present in the adopted volume have been taken as a reference. In this way, a distance distribution function is obtained, in which the atoms occupy stationary positions, which is incorrect, as the atoms vibrate around such positions. In order to consider this fact, each balanced distance was substituted by a Gaussian distance distribution. On the other hand, the RDF thus calculated corresponds to a spherical sample, whereas the experimental RDF was obtained by irradiating a flat sample. In order to make both functions converge, the experimental RDF was modified as proposed by Mason [33], making both RDFs comparable.

The RDF calculated for the initial model will obviously not satisfactorily approach the experimental RDF, so we proceeded to the model refining process, which basically consists of eliciting a positional variation in a given module, in a randomly chosen direction and a randomly chosen atom. The new position is accepted if, respecting the restrictions imposed in the initial configuration, derived from the RDF analysis, the new calculated RDF improves its approximation to the experimental RDF, for example through an evaluation of the mean square deviation between them. The displacement module is determined by taking into account its physical meaning, and it is modified throughout the refining process when, for a given value, the mean square deviation between the two RDFs does not noticeably diminish.

The structural model obtained after the refining process supposes, in any case, a static atomic distribution, and the positions found for the atoms after refining must be considered as average positions around which the corresponding atoms oscillate in amplitudes depending on temperature.

The thermal agitation effect is taken into account, according to the Debye–Waller model, including the thermal factor in the intensity in electronic units.

For the alloy under study, 200 initial positions were generated, included in a 1 nm radius spherical volume,

then eliminating the positions with the lowest coordination, leaving the exact number of atoms of each element, compatible with the formulated hypotheses. The elements Se and Te were assigned coordination two, and As was assigned coordination four; however, in the later refining process, the latter was allowed to break some of its bonds and reduce to coordination three.

The model refining process was begun with movements of 0.05 nm and after 220 valid movements, the square deviation between the RDF of the model and the experimental RDF was 0.0539; the movements were then reduced to an amplitude of 0.03 nm. After 254 movements, the square deviation was 0.0395, and practically constant in the last ten, so it was decided to reduce the atomic movements to 0.01 nm. Once 350 movements were done, the square deviation was 0.029, and the time used to find a valid movement was very long, so it was decided to go on to refining the thermal factors, after which the square deviation was reduced to 0.028.

Fig. 7 shows the experimental and model reduced radial distribution functions, and Table IV shows the initial atomic configuration and the final configuration of the generated model.

Fig. 8 shows a spatial view of the proposed model, from which the bond distances between the different atoms were deduced, as shown in Table V, as well as the average bond angles for each element in the alloy, as shown in Table VI.

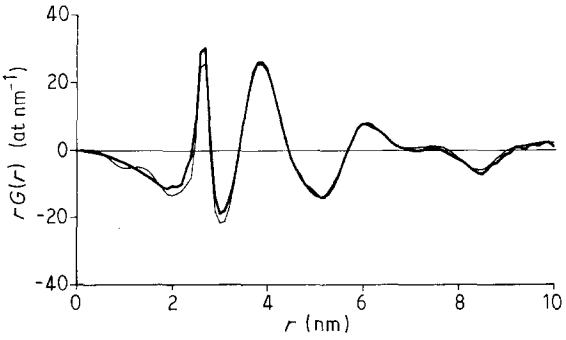

Figure 7 Representation of experimental (——) and calculated (——) RDFs.

TABLE IV Initial and final atomic configuration of the generated model

Element	Coordination	Number of atoms		
		Initial configuration	Final configuration	Total
As	4	26	10	
	3	—	16	26
Se	3	29	13	
	2	7	16	
	1	3	8	
	0	—	2	39
Te	3	10	15	
	2	45	33	
	1	10	14	
	0	—	3	65

TABLE V Averaged bonding distances (nm)

Pair	Bond length	
	This work	Literature
As–As	0.259	0.254 [35]
		0.255 [34]
		0.259 [36]
As–Se	0.248	0.246 [37]
		0.249 [38]
As–Te	0.256	0.261 [35]
		0.255 [38]
Se–Se	0.244	0.244 [37]
		0.245 [38]
Se–Te	0.255	0.258 [37]
Te–Te	0.265	0.262 [35]
		0.267 [34]

TABLE VI Averaged bonding angles (deg.)

Atom	As	Se	Te
Bond angle	110	113	109

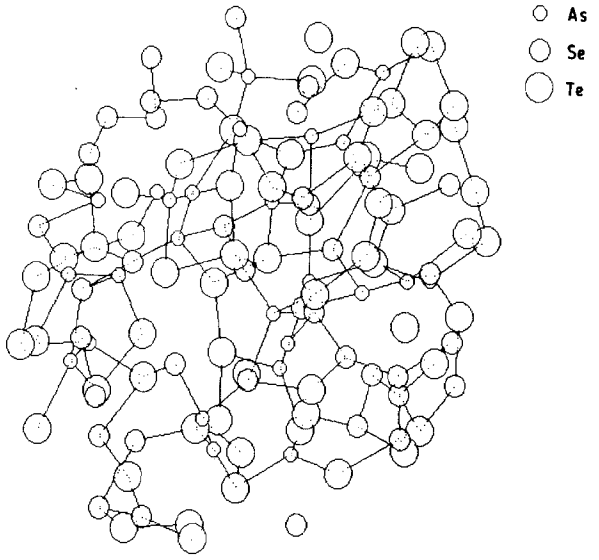

Figure 8 Spatial representation of the model of alloy.

It is important to note that, as is typical of the Glasses manufacturing method, obvious dangling bonds appear in the proposed model. All the infra-coordinated Se atoms are located one bond length away from the surface limit of the model, so they may be considered to be joined to other atoms outside it. The same is true of 70% of the corresponding Te atoms.

As to the bond distances deduced from the model, a good agreement is observed with those quoted in the literature for the same atomic pairs, in alloys similar to the one under study, as reported in Table V.

6. Conclusions

The percentages of infra-coordinated atoms which are near the spherical surface of the model and which may

be saturated with atoms outside it, as well as the average bond angles and the average bond distances deduced for the different pairs of atoms, in relation to the values quoted for them in the literature, in analogous glassy alloys, allow us to state that the generated model is a good statistical representation of the analysed sample, thus confirming the validity of the Metropolis–Monte Carlo method for the generation of atomic structure models in alloys of chalcogenide glasses.

The value found for the area under the first experimental RDF peak made it possible to establish criteria as to the compatibility with the theoretical areas under the same peak, deduced from the tri- and tetra-coordinated As hypotheses.

Both hypotheses are accepted by these criteria, and this is confirmed by the structural model obtained, in which one may observe basic units made up of tetrahedrons centred on tetra-coordinated As atoms, and triangular pyramids, in one of whose vertices there is a tri-coordinated As atom.

These basic units are joined together directly, or by analogous pyramidal units based on Se or Te atoms. Lateral chains, made up of bi-coordinated Se and Te atoms, are also observed to connect the mentioned basic units.

Acknowledgements

The authors are grateful to Aurora Rice for translating this paper into English, and to the Comisión Interministerial de Ciencia y Tecnologia for their financial support (Project No. PB88-0463).

References

1. M. G. BRITTON, *Phys. Technol.* **12** (1981) 187.
2. K. MORJANI and J. M. D. COEY, "Magnetics Glasses" (Elsevier, New York, 1984).
3. A. E. OWEN, in "Electronic and Structural Properties of Amorphous Semiconductors", edited by P. G. Le Comber and J. Mort (Academic, London 1973).
4. D. TURNBULL, *Contemp. Phys.* **10** (1969) 473.
5. R. A. LIGERO, PhD Thesis. University of Cádiz, Spain (1988).
6. J. S. BERKES, Non-Crystalline Solids, 4th International Conference (1977) p. 405.
7. R. A. LIGERO, J. VÁZQUEZ, P. VILLARES and R. JIMÉNEZ-GARAY, *Thermoch. Acta.* in press.
8. J. WASEDA, "The Structure of Non-Crystalline Materials." (McGraw-Hill, New York, 1980).
9. B. E. WARREN, "X-ray Diffraction" (Addison-Wesley, Reading, MA, 1969).
10. R. L. MOZZI and B. E. WARREN, *J. Appl. Crystallogr.* **2** (1969) 164.
11. L. V. AZAROFF, *Acta Crystallogr.* **8** (1955) 701.
12. B. E. WARREN and R. L. MOZZI, *ibid.* **21** (1966) 459.
13. "International Tables of X-ray Crystallography". Vol. III. (Kynoch Press, Birmingham).
14. B. E. WARREN and R. L. MOZZI, *J. Appl. Crystallogr.* **9** (1975) 674.
15. N. J. SHEVCHICK, PhD Thesis, Harvard University, MA (1972).
16. J. VÁZQUEZ and F. SANZ, *Ann. Fis. B* **80** (1984) 31.
17. J. VÁZQUEZ, P. VILLARES and R. JIMÉNEZ-GARAY, *J. Mater. Sci. Lett.* **4** (1986) 485.
18. J. VÁZQUEZ, L. ESQUIVIAS, P. VILLARES and R. JIMÉNEZ - GARAY, *Ann. Fis. B* **81** (1985) 223.
19. G. N. GREAVES and E. A. DAVIS, *Phil. Mag.* **29** (1974) 1201.
20. L. PAULING, "Uniones químicas" (Kapelusz, Buenos Aires, 1969).
21. L. ESQUIVIAS and F. SANZ, *J. Non-Cryst. Solids* **70** (1985) 221.
22. A. D'ANJOU and F. SANZ, *ibid.*, **28** (1978) 319.
23. D. L. PRICE, M. MISAWA, S. SUSMAN, T. I. MORRISON, G. R. SHENOG and M. GRIMADICH, *ibid.* **66** (1984) 443.
24. Z. U. BORISOVA, "Glassy Semiconductors" (Plenum, New York, 1981).
25. J. K. FITZPATRICK and C. MAGHRABI, *Phys. Chem. Glasses* **12** (1971) 105.
26. L. CERVINKA and A. HRUBY, *J. Non-Cryst. Solids* **48** (1982) 231.
27. K. SUZUKI and M. MISAWA, "Liquids Metals", edited by R. Evans and P. A. Creenwood (1976) 531.
28. D. E. POLK, *J. Non-Cryst. Solids* **5** (1971) 365.
29. F. LANCON, L. BILLARD, J. LONGIER and A. CHAMBEROD, *J. Phys. F* **12** (1982) 259.
30. L. BILLARD, F. LANCON and A. CHAMBEROD, *J. Non-Cryst. Solids* **51** (1982) 291.
31. M. D. RECHTIN, A. L. RENNINGER and B. L. AVERBACH, *ibid.* **15** (1974) 74.
32. A. L. RENNINGER, M. D. RECHTIN and B. L. AVERBACH, *ibid.* **16** (1974) 1.
33. G. MASON, *Nature* **217** (1968) 733.
34. R. A. LIGERO, J. VÁZQUEZ, P. VILLARES and R. JIMÉNEZ-GARAY, *J. Mater. Sci. Lett.* **5** (1987) 301.
35. *Idem., J. Mater. Sci.* **23** (1988) 1598.
36. A. J. APLING, A. J. LEADBETLER and A. E. WRIGHT, *J. Non-Cryst. Solids* **23** (1977) 369.
37. J. VÁZQUEZ, E. MÁRQUEZ, P. VILLARES and R. JIMÉNEZ-GARAY, *J. Mater. Sci. Lett.* **4** (1986) 360.
38. J. VÁZQUEZ, P. VILLARES and R. JIMÉNEZ-GARAY, *J. Non-Cryst. Solids* **86** (1986) 251.

Received 18 October 1990
and accepted 25 March 1991